

Order parameter equations for front transitions: Planar and circular fronts

A. Hagberg*

Center for Nonlinear Studies and T-7, Theoretical Division, Los Alamos National Laboratory, Los Alamos, New Mexico 87545

E. Meron†

The Jacob Blaustein Institute for Desert Research and the Physics Department, Ben-Gurion University, Sede Boker Campus 84990, Israel

I. Rubinstein and B. Zaltzman

The Jacob Blaustein Institute for Desert Research and the Mathematics Department, Ben-Gurion University, Sede Boker Campus 84990, Israel

(Received 7 June 1996; revised manuscript received 20 December 1996)

Near a parity breaking front bifurcation, small perturbations may reverse the propagation direction of fronts. Often this results in nonsteady asymptotic motion, such as breathing and domain breakup. Exploiting the time scale differences of an activator-inhibitor model and the proximity to the front bifurcation, we derive equations of motion for planar and circular fronts. The equations involve a translational degree of freedom and an order parameter describing transitions between left and right propagating fronts. Perturbations, such as a space dependent advective field or uniform curvature (axisymmetric spots), couple these two degrees of freedom. In both cases this leads to a transition from stationary to oscillating fronts as the parity breaking bifurcation is approached. For axisymmetric spots, two additional dynamic behaviors are found: rebound and collapse. [S1063-651X(97)09904-2]

PACS number(s): 05.70.Fh, 82.20.Mj, 05.45.+b

I. INTRODUCTION

Pattern dynamics in reaction-diffusion systems often involve nonsteady front motions. These motions can be driven by curvature [1,2], front interactions [3,4], convective instabilities [5,6], and external fields [7–9]. In some cases, fronts reverse their direction of propagation, as, for example, in breathing pulses [10–18], where the reversal is periodic in time, and nucleation of spiral-vortex pairs, where the reversal is local along the extended front line [19–23].

Earlier studies demonstrated that front reversals, as described above, become feasible near a nonequilibrium Ising-Bloch (NIB) bifurcation [15,24], that is, a parity breaking bifurcation where a single stationary front loses stability to a pair of new, counterpropagating fronts. The reversal phenomenon can be regarded as a dynamic transition between the left and right propagating fronts that appear beyond the front bifurcation. It is induced by intrinsic perturbations, like curvature and front interactions [19,25], or weak space dependent external fields [20]. Since the left and right propagating fronts differ in internal structure [15], such a transition involves a new degree of freedom, in addition to the translation mode: the order parameter associated with the bifurcation [20]. The effect of the perturbations is to couple these two degrees of freedom in a way that allows for front reversal.

Our objective is to derive equations for front motion that capture front reversal. Progress toward that goal has already been made in Refs. [20,26] for a nondiffusing inhibitor.

Since inhibitor diffusion is essential for spontaneous front reversals induced by curvature, in this work we study the more difficult case of a diffusing inhibitor. This calls for a different approach as described in Secs. III and IV. In Sec. V we study front reversals induced by two types of perturbations of planar fronts, an external advective field and uniform curvature. In this case, only planar and circular fronts are studied; the derivation of the more general equations for non-uniformly curved fronts can be found in Ref. [27]. Some of the results presented here have been briefly reported in Ref. [28].

II. REACTION-DIFFUSION MODEL

The model we consider is an activator-inhibitor reaction-diffusion system describing a bistable medium. Models of this type have been studied in various physical and chemical contexts [1,2,29–32]. The specific form chosen here is

$$u_t = \epsilon^{-1}(u - u^3 - v) + \delta^{-1}u_{xx}, \quad (1)$$

$$v_t = u - a_1 v + v_{xx}.$$

The variables u and v are scalar real fields representing the activator and the inhibitor, respectively, with the subscripts x and t denoting partial derivatives with respect to these variables. For $a_1 > 1$ system (1) has two stationary uniform states, $(u_{\pm}, v_{\pm}) = (\pm \sqrt{1 - 1/a_1}, \pm a_1^{-1} \sqrt{1 - 1/a_1})$. Note that the parity symmetry $(u, v) \rightarrow (-u, -v)$ of Eqs. (1) is reflected in these solutions. Generalizations of Eqs. (1) to non-symmetric forms in one and two space dimensions will be considered in Sec. V.

*Electronic address: aric@lanl.gov

†Electronic address: ehud@bgumail.bgu.ac.il

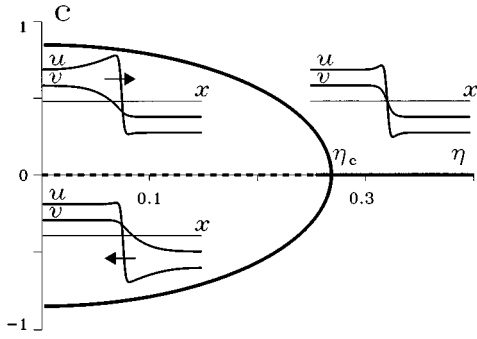


FIG. 1. The NIB (or nonequilibrium Ising-Bloch) bifurcation and internal structure of front solutions. The pitchfork diagram represents the speed of front solutions vs the parameter η . For $\eta > \eta_c$, the Ising front is the single solution and v_f , the order parameter representing the value of the v field at the front position $u=0$, is zero. Beyond the bifurcation, $\eta < \eta_c$, a pair of counter-propagating Bloch fronts appears. The order parameter v_f is negative (positive) for rightward (leftward) propagating fronts.

In addition to the spatially uniform solutions there are also front solutions connecting them. In the following we will consider front solutions that connect (u_+, v_+) at $x = -\infty$ to (u_-, v_-) at $x = \infty$. The number and type of these front solutions is determined by the two parameters ϵ and δ . For $\eta > \eta_c = 3/2\sqrt{2}q^3$, where $\eta = \sqrt{\epsilon\delta}$ and $q^2 = a_1 + 1/2$, a single stable stationary (Ising) front solution exists. This solution loses stability in a pitchfork bifurcation, at $\eta = \eta_c$, to a pair of counterpropagating (Bloch) front solutions [15,31–33] as shown in Fig. 1. The two Bloch front solutions differ not only in their propagation direction but in their internal structure. This difference can be represented by an order parameter associated with the bifurcation, which for $\mu = \epsilon/\delta \ll 1$ can be taken to be the value v_f of the v field at the front position. For simplicity we define the front position to be at $u=0$. With this choice, $v_f=0$ for the Ising front (the inset for $\eta > \eta_c$ in Fig. 1). Beyond the front bifurcation, v_f is nonzero and the sign indicates the direction of front propagation: $v_f < 0$ for the front propagating to the right and $v_f > 0$ for the front propagating to the left ($\eta < \eta_c$ in Fig. 1).

III. FORMULATION OF THE FREE BOUNDARY PROBLEM

In the following we confine ourselves to the region $\epsilon \ll 1$, $\delta \propto \epsilon^{-1}$ and we choose δ values such that $\epsilon\delta \sim \mathcal{O}(\eta_c^2)$. The small parameter ϵ allows the use of singular perturbation methods to study front solutions to Eqs. (1). The first step is to transform to a moving coordinate frame, $x \rightarrow r = x - x_f(t)$, $t \rightarrow t$, where x_f is the position of the front. In this frame Eqs. (1) become

$$u_t - \dot{x}_f u_r = \epsilon^{-1}(u - u^3 - v) + \delta^{-1}u_{rr}, \quad (2)$$

$$v_t - \dot{x}_f v_r = u - a_1 v + v_{rr},$$

where the dot over x_f denotes the derivative with respect to t . The front solution, $u(r, t)$, $v(r, t)$, is characterized by a strong variation of the u field over a distance of order

$\sqrt{\mu} = \sqrt{\epsilon/\delta}$. Stretching the spatial coordinate, $z = r/\sqrt{\mu}$, to expand this region Eqs. (2) become

$$\epsilon(u_t - \dot{z}_f u_z) = u - u^3 - v + u_{zz}, \quad (3)$$

$$\mu(v_t - \dot{z}_f v_z - u + a_1 v) = v_{zz},$$

where $z_f = \dot{x}_f/\sqrt{\mu}$ and we recall that $\mu \propto \epsilon^2$. Expanding in ϵ

$$u = u_0 + \epsilon u_1 + \epsilon^2 u_2 + \dots,$$

$$v = v_0 + \epsilon v_1 + \epsilon^2 v_2 + \dots,$$

and inserting into Eq. (3) we find at order unity the front solution

$$u_0 = -\tanh(z/\sqrt{2}), \quad v_0 = 0.$$

Collecting terms of order ϵ gives

$$\mathcal{L}u_1 = v_1 - \dot{z}_f u_{0z}, \quad \mathcal{L} = \partial_z^2 + 1 - 3u_0^2, \quad (4)$$

where v_1 is a yet undetermined function of time. Since

$$\mathcal{L}u_{0z} = 0,$$

solvability of Eq. (4) requires

$$\dot{z}_f = -\frac{3}{\sqrt{2}}v_1(t).$$

The narrow front region becomes infinitely thin in the limit $\epsilon \rightarrow 0$. Therefore, $v(t)$ may be associated with the value of $v(r, t)$ at the front position, that is $v(0, t)$. With this notation the leading order relation is

$$\dot{x}_f = -\frac{3}{\eta\sqrt{2}}v(0, t). \quad (5)$$

Away from x_f , $u - u^3 - v \sim \mathcal{O}(\epsilon)$, and u varies on the same time and length scales as v . Going back to Eqs. (2), we find at order unity

$$v_t - \dot{x}_f v_r = u_+(v) - a_1 v + v_{rr}, \quad r \leq 0, \quad (6)$$

$$v_t - \dot{x}_f v_r = u_-(v) - a_1 v + v_{rr}, \quad r \geq 0,$$

where $u_{\pm}(v)$ are the outer solution branches of the cubic equation $u - u^3 - v = 0$. For a_1 sufficiently large we may linearize the branches $u_{\pm}(v)$ around $v = 0$

$$u_{\pm}(v) \approx \pm 1 - v/2. \quad (7)$$

Substituting the linearization (7) and the relation from the inner problem (5) into Eq. (6) produces the free boundary problem

$$\left. \begin{aligned} v_t + q^2 v - v_{rr} &= 1 - \frac{3}{\eta\sqrt{2}}v(0, t)v_r \\ v(-\infty, t) &= v_+ \approx q^{-2} \end{aligned} \right\} r \leq 0, \quad (8)$$

$$\left. \begin{aligned} v_t + q^2 v - v_{rr} &= -1 - \frac{3}{\eta\sqrt{2}} v(0,t) v_r \\ v(\infty, t) &= v_- \approx -q^{-2} \end{aligned} \right\} r \geq 0, \quad (9)$$

$$[v]_{r=0} = [v_r]_{r=0} = 0,$$

where the square brackets in Eq. (9) denote jumps across the free boundary. The solution to Eq. (8) leads to a dynamic equation for $v_f(t) = v(0,t)$, the value of the inhibitor at the front position $x_f(t)$, which will complement Eq. (5).

IV. SOLUTION OF THE FREE BOUNDARY PROBLEM

Near the front bifurcation (η close to η_c), the front speed c is small and propagating front solutions can be expanded as power series in c around the stationary front solution. The stationary front solution satisfies the boundary value problem

$$\left. \begin{aligned} v_{rr} - q^2 v + 1 &= 0 \\ v(-\infty) &= q^{-2} \\ v(0) &= 0 \end{aligned} \right\} r \leq 0, \quad (10)$$

$$\left. \begin{aligned} v_{rr} - q^2 v - 1 &= 0 \\ v(\infty) &= -q^{-2} \\ v(0) &= 0 \end{aligned} \right\} r \geq 0,$$

with $[v_r]_{r=0} = 0$. The solution to Eq. (10) is

$$v^{(0)}(r) = q^{-2}(1 - e^{qr}), \quad r \leq 0, \quad (11)$$

$$v^{(0)}(r) = q^{-2}(e^{-qr} - 1), \quad r \geq 0.$$

Note that $v_r^{(0)} = -q^{-1} \exp(-q|r|)$ is not differentiable at $r=0$.

In terms of the deviation from the stationary solution, $\bar{v} = v - v^{(0)}$, Eqs. (8) are

$$\bar{v}_t + q^2 \bar{v} - \bar{v}_{rr} = -\frac{3}{\eta\sqrt{2}} v(0,t) (\bar{v}_r + v_r^{(0)}), \quad (12)$$

$$\bar{v}(\pm\infty) = 0.$$

We seek propagating solutions of Eq. (12) that involve two time scales, the original time t and a slow time $T = c^2 t$. The slow time dependence is a result of the slow evolution of v_f (the value of the inhibitor at the front position) near the front bifurcation. It is easy to show that to linear order $\dot{v}_f \propto (\eta_c - \eta) v_f$ and for a pitchfork bifurcation $\eta_c - \eta \propto c^2$, hence the c^2 scale. Expanding $\bar{v}(r, t, T)$ in powers of c and η in powers of c^2 (expecting a pitchfork bifurcation),

$$\bar{v}(r, t, T) = \sum_{n=1}^{\infty} c^n v^{(n)}(r, t, T), \quad (13)$$

$$\eta = \eta_c - c^2 \eta_1 + c^4 \eta_2 + \dots, \quad (14)$$

and inserting in Eq. (12) gives the sequence of equations

$$v_t^{(n)} + q^2 v^{(n)} - v_{rr}^{(n)} = -\rho^{(n)}, \quad n = 1, 2, 3 \quad (15)$$

where

$$\rho^{(1)} = \frac{3}{\sqrt{2} \eta_c} v|_{r=0}^{(1)} v_r^{(0)}, \quad (16a)$$

$$\rho^{(2)} = \frac{3}{\sqrt{2} \eta_c} [v|_{r=0}^{(1)} v_r^{(1)} + v|_{r=0}^{(2)} v_r^{(0)}], \quad (16b)$$

$$\rho^{(3)} = v_r^{(1)} + \frac{3 \eta_1}{\sqrt{2} \eta_c^2} v|_{r=0}^{(1)} v_r^{(0)}$$

$$+ \frac{3}{\sqrt{2} \eta_c} [v|_{r=0}^{(1)} v_r^{(2)} + v|_{r=0}^{(2)} v_r^{(1)} + v|_{r=0}^{(3)} v_r^{(0)}]. \quad (16c)$$

Equation (15) can be solved using an appropriate Green's function and assuming that the front motion is independent of the fast time scale t as $t \rightarrow \infty$ [28]. A simplified derivation of the solution follows from the gradient nature of Eq. (15) when the source term $\rho^{(n)}(r, T)$ becomes independent of t . For then $v_t^{(n)} \rightarrow 0$ as $t \rightarrow \infty$ for any r and we can look for stationary (t independent) solutions.

Consider first $v^{(1)}$. Inserting Eq. (16a) in $v_{rr}^{(1)} - q^2 v^{(1)} = \rho^{(1)}$ and solving for $v^{(1)}$ we obtain

$$v^{(1)}(r, T) = \frac{3}{2\sqrt{2} \eta_c q^3} v^{(1)}(0, T) F(r), \quad (17)$$

where

$$F(r) = (1 - qr) e^{qr}, \quad r \leq 0,$$

$$F(r) = (1 + qr) e^{-qr}, \quad r \geq 0.$$

Setting $r=0$ we find

$$\eta_c = \frac{3}{2\sqrt{2} q^3}. \quad (18)$$

The critical value $\eta_c = \eta(c=0)$ determines the bifurcation point where the propagating Bloch front solutions coincide with the stationary Ising front. The expression (18) is the same as the one derived earlier using a different method [15,25].

Using Eq. (17) to solve $v_{rr}^{(2)} - q^2 v^{(2)} = \rho^{(2)}$ we find

$$v^{(2)}(r, T) = [v^{(2)}(0, T) + \frac{1}{2} v^{(1)}(0, T)^2 q^3 r] F(r), \quad (19)$$

and using both Eqs. (17) and (19) in $v_{rr}^{(3)} - q^2 v^{(3)} = \rho^{(3)}$, we obtain

$$\left. \begin{aligned} v^{(3)}(r, T) &= v^{(3)}(0, T) e^{qr} + A_+ r e^{qr} \\ &\quad - B_+ r^2 e^{qr} - C_+ r^3 e^{qr}, \end{aligned} \right\} r \leq 0, \quad (20)$$

$$\left. \begin{aligned} v^{(3)}(r, T) &= v^{(3)}(0, T) e^{-qr} + A_- r e^{-qr} \\ &\quad - B_- r^2 e^{-qr} - C_- r^3 e^{-qr}, \end{aligned} \right\} r \geq 0,$$

where

$$A_{\pm} = q^3 v^{(1)}(0, T) v^{(2)}(0, T) \pm \left[\frac{3}{4q} v_T^{(1)}(0, T) + \frac{1}{2} q^5 v^{(1)}(0, T)^3 - \frac{q \eta_1}{\eta_c} v^{(1)}(0, T) - q v^{(3)}(0, T) \right],$$

$$B_{\pm} = \frac{1}{4} \eta_T^{(1)}(0, T) \pm q^4 v^{(1)}(0, T) v^{(2)}(0, T),$$

$$C_{\pm} = \pm \frac{1}{6} q^7 v^{(1)}(0, T)^3.$$

Application of the (no) jump condition $[v_r^{(3)}]_{r=0} = 0$ leads to

$$\eta_c^2 v_T^{(1)}(0, T) = \frac{\sqrt{2} \eta_1}{q} v^{(1)}(0, T) - \frac{3}{4} v^{(1)}(0, T)^3. \quad (21)$$

Equation (21) still contains an unspecified parameter, η_1 . To identify η_1 recall that c is the speed of a front propagating at constant velocity. From Eq. (5)

$$|\dot{x}_f| = \frac{3}{\sqrt{2} \eta_c} c |v^{(1)}(0, T)| + \mathcal{O}(c^2).$$

Identifying $|\dot{x}_f|$ with c gives $v^{(1)2} = 2 \eta_c^2 / 9$ for a front propagating at constant speed. This value of $v^{(1)2}$ should coincide with the nontrivial stationary solution of Eq. (21), $v^{(1)2} = 4 \sqrt{2} \eta_1 / 3q$. Comparing the two expressions gives

$$\eta_1 = \frac{q \eta_c^2}{6 \sqrt{2}}. \quad (22)$$

Equations (22) and (14) provide the leading order form of the front bifurcation diagram

$$c^2 = \frac{6 \sqrt{2}}{q \eta_c^2} (\eta_c - \eta),$$

which coincides for small c with the earlier result [6,9], $c^2 = 4q^2(\eta_c^2 - \eta^2)/\eta^2$.

Multiplying Eq. (21) by c and using the expansions (13) and (14) gives the equation of motion for propagating fronts

$$\dot{v}_f = \frac{\sqrt{2}}{q \eta_c^2} (\eta_c - \eta) v_f - \frac{3}{4 \eta_c^2} v_f^3, \quad (23a)$$

$$\dot{x}_f = -\frac{3}{\eta \sqrt{2}} v_f, \quad (23b)$$

where the slow time derivative of v_f is expressed in terms of a fast time derivative ($\dot{v}_f = c^2 v_{fT}$).

According to Eqs. (23) the dynamics of a propagating front involve two degrees of freedom: a translational degree of freedom, x_f , determining the front position, and an order parameter, v_f , determining the direction of propagation. The latter has not been appreciated enough since most works to date [1,2] have focused on conditions far from the front bifurcation. In that case the two stationary states, $v_f = \pm [4 \sqrt{2} (\eta_c - \eta) / 3q]^{-1/2}$, representing fronts propagating in opposite directions, are highly stable. Close to the

front bifurcation, however, the eigenvalue associated with these states, $\lambda = -2 \sqrt{2} (\eta_c - \eta) / q$, approaches zero and small disturbances can drive the system from one state to another, thereby inducing *front reversals*.

V. FRONT REVERSAL: OSCILLATIONS AND REBOUND

Equations (23) describe the motion of a freely propagating front in a uniform medium. In this section we show how two different perturbations affect front propagation. The first is the addition of a space dependent advective field to the v equation in the original system (1). This type of differential advection appears for example in chemical reactions involving ionic species that are subjected to electric fields [8,34]. The second is the intrinsic perturbation of uniform curvature variations on the propagation of two dimensional fronts. Both perturbations lead to a coupling of the two degrees of freedom in the order parameter Eqs. (23) and allow for the nonsteady asymptotic motion of fronts.

A. Space dependent advective field

To study the effect of an external advective field J we add the term $J v_x$ to the v equation in Eq. (1),

$$u_t = \epsilon^{-1} (u - u^3 - v) + \delta^{-1} u_{xx}, \quad (24)$$

$$v_t = u - a_1 v - a_0 + J v_x + v_{xx}.$$

The small parameter a_0 is also introduced to break the parity symmetry of Eq. (1). For simplicity we consider a linear spatial profile, $J = -\alpha x$, $0 < \alpha \leq 1$. Proceeding as before, the inner region analysis remains unchanged and culminates in Eq. (23b). The outer analysis leads to the additional terms, $-\alpha(r + x_f) v_r - a_0$, on the right hand side of both partial differential equations in Eq. (8). Assuming $\alpha = \alpha_0 c^3$ and $a_0 = a_{00} c^3$, where α_0 and a_{00} are of order unity, Eqs. (16a) and (16b) remain unchanged, but Eq. (16c) acquires, on the right hand side, two additional terms: $\alpha_0(r + x_f) v_r^{(0)} + a_{00}$. As a result the order parameter Eqs. (23) are changed to

$$\dot{v}_f = \frac{\sqrt{2}}{q \eta_c^2} (\eta_c - \eta) v_f - \frac{3}{4 \eta_c^2} v_f^3 + \frac{2}{3q} \alpha x_f - \frac{4}{3} a_0, \quad (25a)$$

$$\dot{x}_f = -\frac{3}{\eta \sqrt{2}} v_f. \quad (25b)$$

Notice that the introduction of a *space dependent* advective field couples the two degrees of freedom, v_f and x_f . This coupling affects the front behavior in two significant ways: for $\eta > \eta_c$ (and $a_0 \neq 0$) it stabilizes a propagating front at a fixed position, $x_f = 2qa_0/\alpha$, and for $\eta < \eta_c$ it induces oscillations between the counterpropagating fronts. The frequency of oscillations close to the Hopf bifurcation at $\eta = \eta_c$ is

$$\omega = \frac{2}{\sqrt{3}} q \sqrt{\alpha}. \quad (26)$$

We tested the validity of Eqs. (25) by numerically integrating the original system (1) and comparing the oscillating

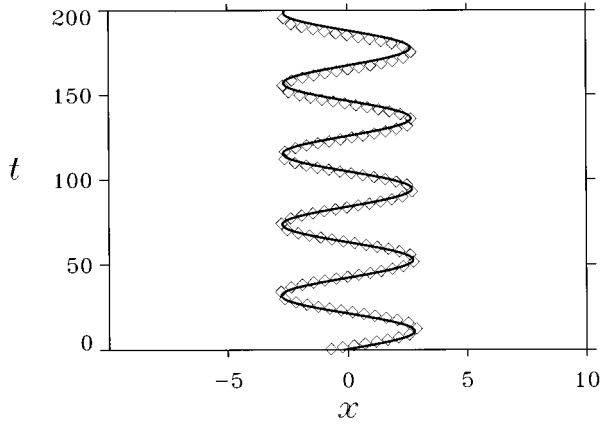


FIG. 2. Front position, x_f , vs time for an oscillating front. The solid line represents the solution to the order parameter equations (25) and the diamonds are from the numerical solution of the original partial differential equations (1). Parameters: $a_1=3.0$, $\epsilon=0.01$, $\delta=2.77$, $a_0=0$, $\alpha=0.005$.

front solutions with those of Eq. (25). The agreement, as Fig. 2 shows, is very good. In Fig. 3 we plotted the frequency of front oscillations vs the field gradient according to Eq. (26) and as obtained from Eq. (1). Again, the agreement is excellent, and remains good even for c of order unity. Note that in the inner analysis we neglected contributions of $\mathcal{O}(\epsilon^2)$ to v at the front position, while in the outer analysis we kept terms to $\mathcal{O}(c^3)$. A quantitative comparison as described above, therefore, requires that c is much larger than $\epsilon^{2/3}$.

B. Uniform curvature

In two space dimensions the reaction-diffusion system (1) becomes

$$u_t = \epsilon^{-1}(u - u^3 - v) + \delta^{-1}\nabla^2 u, \quad (27)$$

$$v_t = u - a_1 v - a_0 + \nabla^2 v,$$

where the small parameter a_0 has been added again to break the parity symmetry of Eq. (1). In addition to planar front

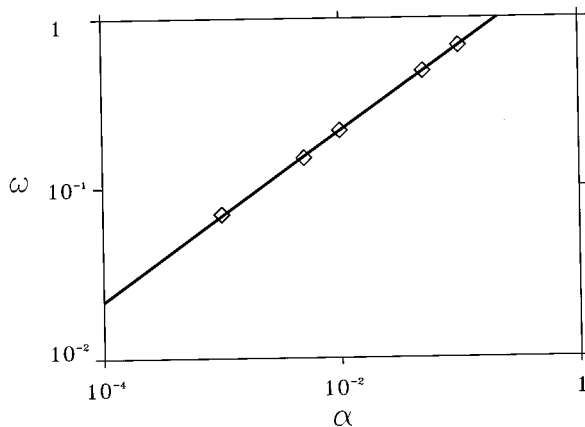


FIG. 3. A log-log plot of the oscillation frequency ω vs the external field gradient α . The solid line is the relation of Eq. (26) and the diamonds represent numerical solutions of Eqs. (1). Parameters: $a_1=3.0$, $\epsilon=0.01$, $\delta=2.77$, $a_0=0$.

solutions, there are now new types of solutions, including fronts with uniform curvature (circular fronts or spots). These spots may be stationary or, for parameters near a NIB bifurcation, may collapse, expand indefinitely, or oscillate periodically in time.

To derive equations for the motion of circular fronts, the first step is to transform into polar coordinates, $r = \rho - \rho_f(t)$, that move with the front. In this frame and assuming the radius of curvature ρ_f is much larger than the front width, Eqs. (27) are

$$u_t - (\dot{\rho}_f + \delta^{-1}\kappa)u_r = \epsilon^{-1}(u - u^3 - v) + \delta^{-1}u_{rr},$$

$$v_t - (\dot{\rho}_f + \kappa)v_r = u - a_1 v - a_0 + v_{rr},$$

where $\kappa = \rho_f^{-1}$ is the front curvature. As before we assume $\epsilon \ll 1$ and $\delta \propto \epsilon^{-1}$ and use singular perturbation theory.

Analysis of the inner, or front, region yields a relation analogous to Eq. (23b)

$$\dot{\rho}_f + \delta^{-1}\kappa = -\frac{3}{\eta\sqrt{2}}v_f. \quad (28)$$

In the outer region, instead of Eq. (8) we must solve

$$v_t + q^2 v - v_{rr} = \pm 1 - \frac{3}{\eta\sqrt{2}}v(0,t)v_r + P,$$

where $P = (1 - \delta^{-1})v_r/\rho_f - a_0$. Assuming that P is a small perturbation (of order $|c|^3$) and proceeding as in Sec. IV we obtain the order parameter equation

$$\dot{v}_f = \frac{\sqrt{2}}{q\eta_c^2}(\eta_c - \eta)v_f - \frac{3}{4\eta_c^2}v_f^3 - \frac{2}{3q}\frac{(1 - \delta^{-1})}{\rho_f} - \frac{4}{3}a_0. \quad (29)$$

Writing Eqs. (28) and (29) in terms of the curvature $\kappa = \rho_f^{-1}$ gives the equations

$$\dot{v}_f = \frac{\sqrt{2}}{q\eta_c^2}(\eta_c - \eta)v_f - \frac{3}{4\eta_c^2}v_f^3 - \frac{2}{3q}(1 - \delta^{-1})\kappa - \frac{4}{3}a_0, \quad (30a)$$

$$\dot{\kappa} = \frac{3}{\eta\sqrt{2}}v_f\kappa^2 + \delta^{-1}\kappa^3, \quad (30b)$$

that describe the dynamics of large circular spots. The introduction of curvature *couple*s the two equations. Equations (23), for planar fronts, are decoupled and only describe the relaxation to steadily propagating fronts. The equations for circular fronts additionally allow front reversals and non-steady asymptotic motion such as oscillations.

Consider first the fixed point solutions obtained by the intersections of the linear nullclines $\kappa=0$ and $\kappa = -(3\delta/\eta\sqrt{2})v_f$ of Eq. (30b) with the cubic nullcline of Eq. (30a). The solutions corresponding to $\kappa=0$ describe planar fronts propagating at constant velocities. Solutions with positive and negative v_f values pertain to down states invading up states and up states invading down states, respectively. The number of $\kappa=0$ solutions varies with η . Below

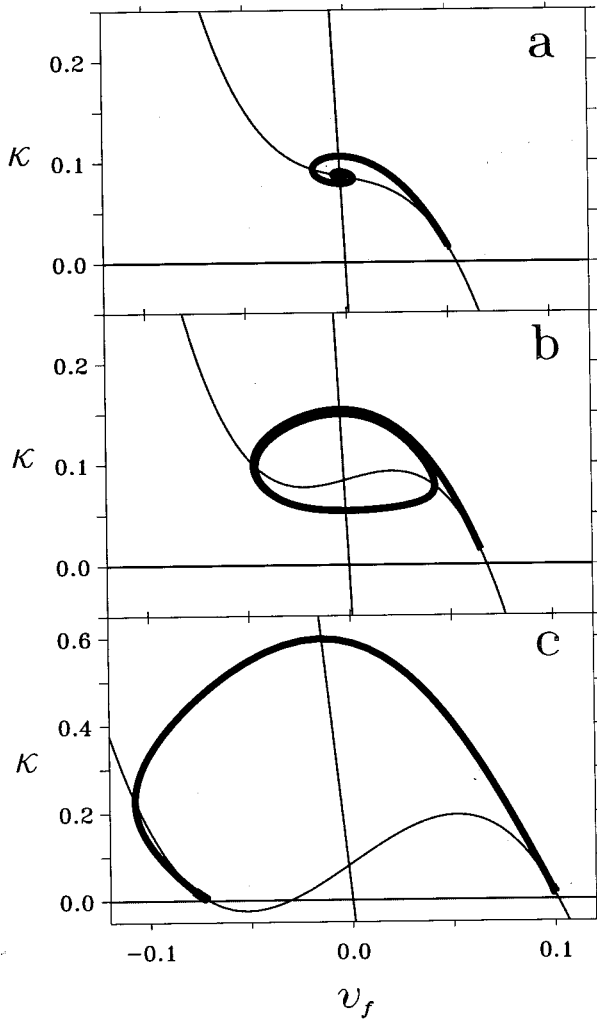


FIG. 4. Three types of solutions to the order parameter equations (30) starting with initial conditions representing a large shrinking spot. The thin lines are the isoclines and the thick lines are numerically computed trajectories. (a) Convergence to a stationary spot ($\epsilon=0.0063$). (b) An oscillating spot ($\epsilon=0.006$). (c) Spot rebound and expansion of the spot to infinite size ($\epsilon=0.0052$). Parameters: $a_1=4.0$, $a_0=-0.01$, and $\delta=2.0$.

the front bifurcation, [$\eta > \eta_c(a_0)$], there is a single intersection point representing an Ising front as shown by the thin lines in Figs. 4(a) and 4(b). Beyond the front bifurcation, [$\eta < \eta_c(a_0)$], two more intersection points appear corresponding a stable and unstable pair of planar front solutions [Fig. 4(c)]. The fixed point solutions for $\kappa \neq 0$ represent circular fronts. For $a_0 < 0$ they describe spots of an up state domain and for $a_0 > 0$ spots of a down state domain. For $\delta > 1$, depending on the choice of ϵ , these fixed points may or may not be stable. For $\delta < 1$, all the $\kappa \neq 0$ fixed points are *unstable*.

Figure 4 shows three different possibilities for the dynamics of circular fronts. The thick trajectories represent dynamics computed by numerical solution of the coupled equations (30). The initial conditions correspond to a large shrinking up state spot. Far into the Ising regime [Fig. 4(a)] the initial spot converges to a stationary spot. Moving closer to the front bifurcation and past a critical η value, $\eta_H > \eta_c(a_0)$, a Hopf bifurcation to a breathing spot occurs [Fig. 4(b)].

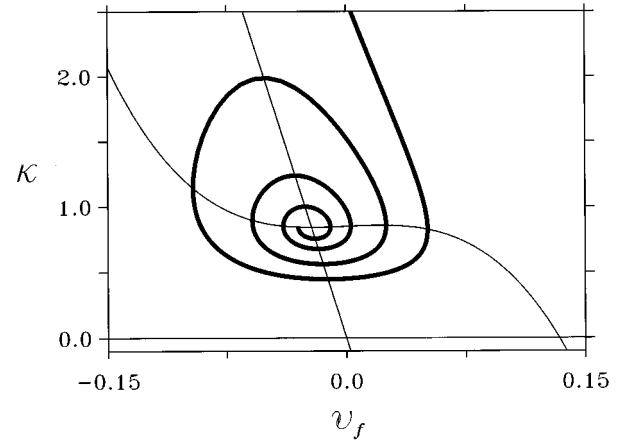


FIG. 5. A trajectory of the order parameter equations (30) for a spot that oscillates with growing amplitude until collapse (the curvature κ diverges to infinity). Parameters: $a_1=4.0$, $a_0=-0.1$, $\epsilon=0.006$, and $\delta=2.0$.

Crossing the front bifurcation, $\eta < \eta_c(a_0)$, the spot rebounds, i.e., the shrinking spot reaches a minimal size and expands again indefinitely [Fig. 4(c)]. For larger $|a_0|$, there is another possibility for the dynamics of spots. In this case, shown in Fig. 5, the amplitude of oscillations grows in time until the spot eventually collapses as the curvature diverges to infinity.

All three behaviors discussed above have been observed in direct numerical solutions of Eq. (27). The quantitative accuracy of the order parameter equations was tested by computing numerical solutions to the circularly symmetric version of Eqs. (27)

$$u_t = \epsilon^{-1}(u - u^3 - v) + \frac{\delta^{-1}}{r}u_r + \delta^{-1}u_{rr}, \quad (31)$$

$$v_t = u - a_1v - a_0 + \frac{1}{r}v_r + v_{rr},$$

and comparing them to solutions of Eqs. (30) for spot dynamics. Spot solutions of Eqs. (31) produce the same qualitative behavior as the pair of coupled equations for the spot dynamics. When the parameters are chosen to satisfy the assumptions made in the derivation of Eqs. (30), there is also quantitative agreement between the two solutions. Figure 6 shows the curvature of an oscillating spot as a function of time computed using both Eqs. (30) and (31). The two solutions agree within an accuracy of approximately 1% for the amplitude and 2% for the phase.

In addition to the oscillatory instability spot, solutions may also be unstable to transverse perturbations [35–37]. Numerical solutions of the fully two-dimensional model (27) show that for the parameters of Fig. 6 spots are unstable and form nonuniformly curved fronts leading to a labyrinthine pattern. Since the order parameter equations derived here apply only for the case when the spots do not break perfect circular symmetry, for this choice of parameters they only capture the dynamics of the circular spot during the initial evolution. Order parameter equations for the dynamics of nonuniformly curved fronts are presented in Ref. [27].

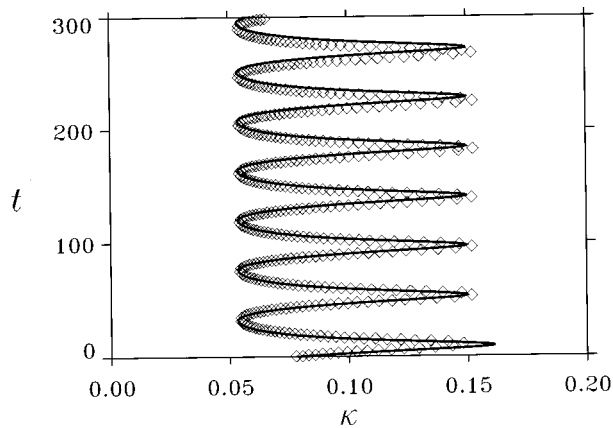


FIG. 6. An oscillating circular spot solution. The solid line is the solution of the order parameter equations (30), and the diamonds represent the spot curvature vs time from the numerical solution to the circularly symmetric equations (31). The equation parameters are $\epsilon=0.006$, $\delta=2.0$, $a_1=4.0$, $a_0=-0.01$.

VI. CONCLUSION

We derived the equations that govern the dynamics of planar fronts in bistable systems near a parity breaking front bifurcation (the NIB bifurcation). In this case the context is an activator-inhibitor model, but the normal form

$$\dot{X} = C, \quad (32)$$

$$\dot{C} = (\alpha_c - \alpha)C - \beta C^3,$$

is general. Here, X is the front position, C is the front velocity, and α_c is a critical parameter value for which a NIB bifurcation occurs. Similar equations should apply, for example, to liquid crystals subjected to rotating magnetic fields [38–40] and have also been proposed in the context of parity breaking traveling-wave bifurcations [41].

Uniform front curvature, or space dependent external fields, couple the two degrees of freedom, X and C , and

allow nonsteady asymptotic behavior. The coupled sets of equations (25) and (30) exhibit Hopf bifurcations from stationary to oscillating fronts (breathing spots). Equations (30) exhibit two additional behaviors pertaining to rebounding and collapsing spots in the full equations.

Curvature effects on front dynamics near a NIB bifurcation were also studied in Refs. [20,25] using a “quasistatic” approximation. This approximation, where the front velocity is assumed to adiabatically follow slow curvature variations [1,2], yields an *algebraic* relation between the front velocity C and its curvature κ . As the bifurcation is approached the $C-\kappa$ relation becomes multivalued, or hysteretic. The multivalued relations correctly predict spontaneous front transitions induced by curvature [20,25], but cannot describe dynamics during front transitions. Differential order parameter equations, like Eqs. (30), give a more accurate characterization of the dynamics. These differential equations reduce to an algebraic $C-\kappa$ relation when the time scale of front transitions becomes much shorter than the time scale of curvature changes. Such a condition is realized, for example, with very large spots away from the front bifurcation. Then the right hand side of Eq. (30a) can be set to zero, an expression which together with Eq. (28) gives an algebraic $C-\kappa$ relation, where $C = \dot{\rho}_f$.

The phenomena of breathing, oscillating, and collapsing spots appear to be quite general and can be induced by other perturbations that couple X and C . Reference [42], which studies the effect of boundaries on spot dynamics, reports on the observation of stationary, breathing, and rebounding spots. Interaction between fronts may similarly lead to stationary, oscillating, and collapsing domains [10–18]. Recent experiments on the ferrocyanide-iodate-sulfite reaction show small oscillating chemical spots away from the reactor boundary that are most likely due to front interactions and/or curvature [43].

ACKNOWLEDGMENTS

This study was supported in part by the Israel Ministry of Science and the Arts.

-
- [1] J. J. Tyson and J. P. Keener, *Physica D* **32**, 327 (1988).
 - [2] E. Meron, *Phys. Rep.* **218**, 1 (1992).
 - [3] C. Elphick, E. Meron, and E. A. Spiegel, *Phys. Rev. Lett.* **61**, 496 (1988).
 - [4] C. Elphick, E. Meron, and E. A. Spiegel, *SIAM J. Appl. Math.* **50**, 490 (1990).
 - [5] K. I. Agladze, V. I. Krinsky, and A. M. Pertsov, *Nature* **308**, 834 (1984).
 - [6] S. C. Müller, T. Plesser, and B. Hess, in *Physiochemical Hydrodynamics: Interfacial Phenomena*, edited by M. G. Velarde (Plenum, New York, 1988).
 - [7] P. Ortoleva, *Physica D* **26**, 67 (1987).
 - [8] O. Steinbock, J. Schütze, and S. C. Müller, *Phys. Rev. Lett.* **68**, 248 (1992).
 - [9] A. F. Munster, P. Hasal, D. Snita, and M. Marek, *Phys. Rev. E* **50**, 546 (1994).
 - [10] S. Koga and Y. Kuramoto, *Prog. Theor. Phys.* **63**, 106 (1980).
 - [11] B. S. Kerner and V. V. Osipov, *Zh. Éksp. Teor. Fiz.* **83**, 2201 (1982) [*Sov. Phys. JETP* **56**, 1275 (1982)].
 - [12] Y. Nishiura and M. Mimura, *SIAM J. Appl. Math.* **49**, 481 (1989).
 - [13] T. Ohta, A. Ito, and A. Tetsuka, *Phys. Rev. A* **42**, 3225 (1990).
 - [14] Y. A. Rzanov, H. Richardson, A. A. Hagberg, and J. V. Moloney, *Phys. Rev. A* **47**, 1480 (1993).
 - [15] A. Hagberg and E. Meron, *Nonlinearity* **7**, 805 (1994).
 - [16] M. Suzuki, T. Ohta, M. Mimura, and H. Sakaguchi, *Phys. Rev. E* **52**, 3645 (1995).
 - [17] C. B. Muratov and V. V. Osipov, *Phys. Rev. E* **53**, 3101 (1996).
 - [18] R. Woesler, P. Schütz, M. Bode, M. Or-Guil, and H.-G. Purwins, *Physica D* **91**, 376 (1996).
 - [19] A. Hagberg and E. Meron, *Phys. Rev. Lett.* **72**, 2494 (1994).
 - [20] C. Elphick, A. Hagberg, and E. Meron, *Phys. Rev. E* **51**, 3052 (1995).

- [21] K. J. Lee, W. D. McCormick, Q. Ouyang, and H. L. Swinney, *Science* **261**, 192 (1993).
- [22] K. J. Lee, W. D. McCormick, J. E. Pearson, and H. L. Swinney, *Nature* **369**, 215 (1994).
- [23] K. J. Lee and H. L. Swinney, *Phys. Rev. E* **51**, 1899 (1995).
- [24] P. Couillet, J. Lega, B. Houchmanzadeh, and J. Lajzerowicz, *Phys. Rev. Lett.* **65**, 1352 (1990).
- [25] A. Hagberg and E. Meron, *Chaos* **4**, 477 (1994).
- [26] M. Bode, *Physica D* (to be published).
- [27] A. Hagberg and E. Meron, *Phys. Rev. Lett.* **78**, 1166 (1997).
- [28] A. Hagberg, E. Meron, I. Rubinstein, and B. Zaltzman, *Phys. Rev. Lett.* **76**, 427 (1996).
- [29] M. Bär, S. Nettesheim, H. H. Rotermund, M. Eiswirth, and G. Ertl, *Phys. Rev. Lett.* **74**, 1246 (1995).
- [30] G. Haas, M. Bär, I. G. Kevrekidis, P. B. Rasmussen, H.-H. Rotermund, and G. Ertl, *Phys. Rev. Lett.* **75**, 3560 (1995).
- [31] M. Bode, A. Reuter, R. Schmeling, and H.-G. Purwins, *Phys. Lett. A* **185**, 70 (1994).
- [32] P. Schütz, M. Bode, and H.-G. Purwins, *Physica D* **82**, 382 (1995).
- [33] H. Ikeda, M. Mimura, and Y. Nishiura, *Nonl. Anal. TMA* **13**, 507 (1989).
- [34] J. J. Taboada, A. P. Muñuzuri, V. Pérez-Muñuzuri, M. Gómez-Gesteira, and V. Pérez-Villar, *Chaos* **4**, 519 (1994).
- [35] T. Ohta, M. Mimura, and R. Kobayashi, *Physica D* **34**, 115 (1989).
- [36] D. M. Petrich and R. E. Goldstein, *Phys. Rev. Lett.* **72**, 1120 (1994).
- [37] R. E. Goldstein, D. J. Muraki, and D. M. Petrich, *Phys. Rev. E* **53**, 3933 (1996).
- [38] S. Nasuno, N. Yoshimo, and S. Kai, *Phys. Rev. E* **51**, 1598 (1995).
- [39] T. Frisch, S. Rica, P. Couillet, and J. M. Gilli, *Phys. Rev. Lett.* **72**, 1471 (1994).
- [40] K. B. Migler and R. B. Meyer, *Physica D* **71**, 412 (1994).
- [41] E. Knobloch, J. Hettel, and G. Dangelmayr, *Phys. Rev. Lett.* **74**, 4839 (1995).
- [42] D. Haim, G. Li, Q. Ouyang, W. D. McCormick, H. L. Swinney, A. Hagberg, and E. Meron, *Phys. Rev. Lett.* **77**, 190 (1996).
- [43] G. Li, Q. Ouyang, and H. L. Swinney, *J. Chem. Phys.* **105**, 10830 (1996).